UDC 620.187:621.039.531

STRUCTURE AND PROPERTIES OF AUSTENITIC ODS STEEL 08Cr18Ni10Ti

A.N. Velikodnyi[1], V.N. Voyevodin[1,2], M.A. Tikhonovsky[1], V.V. Bryk[1], A.S. Kalchenko[1], S.V. Starostenko[1,2], I.V. Kolodiy[1], V.S. Okovit[1], A.M. Bovda[1], L.V. Onischenko[1], G.Ye. Storogilov[1]

[1]National Science Center "Kharkov Institute of Physics and Technology", Kharkov, Ukraine;
[2]V.N. Karazin Kharkov National University, Kharkov, Ukraine
E-mail: velikodnyi@kipt.kharkov.ua

Using mechanical alloying, experimental samples of austenitic stainless steel 08Cr18Ni10Ti dispersion hardening nano systems Y_2O_3-ZrO_2 different composition. The microstructure of samples at various stages of preparation, depending on the composition of an oxide of the alloying conditions and thermal-mechanical processing. Defined structural parameters tape sample (particle size, density and size distribution of the precipitates, etc.). The mechanical properties of tapes at room temperature and at 700 ºC and it is shown that the characteristics ODS steel is significantly higher compared with a conventional steel, obtained according to the same modes. This difference is particularly significant in the test conditions at 700 ºC, where the yield strength of ODS steel is 2.3 times higher than for initial steel 08Cr18Ni10Ti. ODS steel ductility is somewhat lower than the initial one, but its value remains at a level sufficient for the technological and operational goals.

INTRODUCTION

Austenitic steels are used in nuclear power as material for pressure vessel internals and fuel claddings in fast reactors. In comparison with ferritic-martensitic steels they are characterized by higher high-temperature strength, but have lower radiation resistance [1]. The problem solution of the improvement of austenitic steels radiation resistance with simultaneous increasing of high-temperature resistance is possible by the nanostructural state production in these alloys, that characterized by the presence of nanosized particles (~ 2…10 nm) with high density (~ 10^{15}…10^{16}cm^{-3}) and uniform distribution into the matrix. Increase of radiation resistance is caused by the large extent of boundaries "matrix-nanoparticles", which are the effective sinks for radiation defects [2-4]. Thermodynamically stable oxides may serve as such nanoparticles and steels, strengthened by such particles are named oxide dispersion-strengthened steels (ODS steels).

Traditional method of ODS steel production includes the mechanical alloying (MA) of steel powders by nanosized oxides (mechanical alloying) with their subsequent compacting and mechanical-thermal treatment [5-7]. During the mechanical alloying process oxide dissolves (partially or completely) in the steel matrix and during subsequent mechanical-thermal treatment of compacted materials precipitation of secondary nanosized particles of oxide occurs. Composition of precipitated particles mostly doesn't coincide with the initial oxide composition. Yttrium oxide nanopowder [5, 7] is used as oxide more often but there are also some examples of other oxides, aluminum oxides for example [8]. Oxide composition either as presence of alloying elements with high affinity for oxygen (titanium, for example) in steel has significant influence on properties and structure formation of ODS steels.

The goal of this paper was to study the influence of yttria-doped zirconia nanopowders composition and conditions of steel manufacturing on structure and mechanical properties of stainless steel 18Cr10NiTi.

MATERIALS AND METHODS

Commercial austenitic steel 08Cr18Ni10Ti was used as initial steel. Material for mechanical alloying was prepared by two methods.

The first method includes melting of initial steel specimens in vacuum and pouring out of the molten alloy on rotating water-cooled copper wheel (melt-spinning) [9].

Using such treatment the 20 μm thick melt-spun ribbons were obtained in highly non-equilibrium state. It was assumed, that the small thickness of the ribbons and its non-equilibrium state allow accelerate the process of steel mechanical alloying by oxides.

In the second method the steel powders were obtained by mechanical grinding by abrasives. Screening of the powder was performed; the powder of less than 300 μm size and close to the equiaxial shape was used for mechanical alloying.

Ribbon fragments with dimensions 3x3 mm or the initial steel powder were mixed with 0.5%wt of oxide nanopowder produced by Don PhTI NANU (Donetsk) and mechanically alloyed in argon in high-energy ball mill (rotation rate was 480 rpm) during 1…10 hours. The balls made of steel SHKH13 and with of different diameters were used. Obtained powder consisted of agglomerated particles with multi modal distribution and substantial size distribution within the range of some μm to 500 μm and more. Further fraction with the size less than 300 μm was used in our work.

All kinds of mechanical treatment from powder compacting to rolling of compacted blank were carried out at room temperature. In addition, mechanical treatments were alternated with short-time annealing in vacuum at temperature 1200 °C. In the result the bands of ODS steel 08Cr18Ni10Ti with thickness 200 μm were obtained.

The specimen structure analysis was conducted by the methods of electron microscopy using JEM-100CX and JEM-2100 microscopes.

X-ray diffraction study was performed by DRON-2 diffractometer using Fe-Kα radiation. All specimens were measured under the same conditions. Since the diffraction lines from powder specimens had week intensity the diffraction patterns were collected not in wide angular range but by selected interval. After this the preliminary treatment of diffraction patterns was carried out (background subtraction, smoothing, $K\alpha_2$ reduction) and approximation of diffraction lines with pseudo-Voigt function. Quantitative phase analysis was performed by relation intensity ratio method (RIR). Microstructural study (size-strain analysis) was conducted by single line method [10].

RESULTS AND DISCUSSION

INITIAL MATERIALS PARAMETERS

Initial steel microanalysis showed (Fig. 1), that its composition by main elements complies with State standard GOST 5632-72. Characteristics of used oxide nanopowders are presented in Tabl. 1.

Element	Content, wt.%	Content, at.%
Si K	0.41	0.81
Ti K	0.63	0.72
Cr K	18.90	20.01
Mn K	1.63	1.62
Fe K	67.51	66.60
Ni K	10.76	10.10
Cu K	0.16	0.14
Total	100.00	100.00

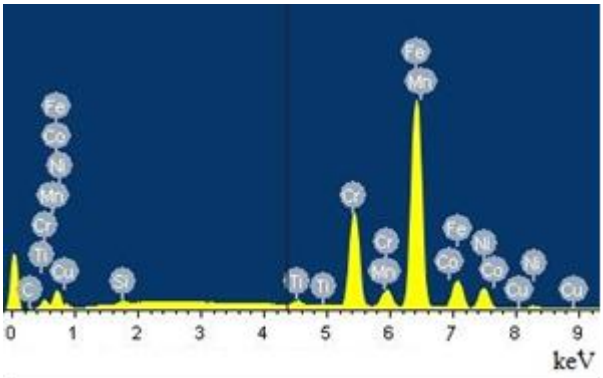

Fig. 1. Composition of steel according to microanalysis data

Table 1

Parameters of nanopowders of system Y_2O_3-ZrO_2

Y_2O_3 Content, mol.%	Particle size* (crystallite size), nm	Lattice parameter, *a***, Å
80	16.5	$10.528\pm8\cdot10^{-3}$
20	29.0	$5.208\pm3\cdot10^{-3}$
8	14.3	$5.132\pm2\cdot10^{-3}$

** Firm-supplier data, ** current work data.*

As it can be seen from Tabl. 1 all powders have cubic lattice, powder size for different yttria content varies from 14 to 29 nm.

CHARACTERISTICS OF STEEL POWDERS, MECHANICALLY ALLOYED BY NANOOXIDES

As it was seen from investigation, increasing the time of grinding in inert medium leads to the better solution of oxide powders in steel matrix. On the other hand, it is observed the increasing of powder fraction, which alloys mechanically with formation of round-shape particles more than 500 μm size or adheres to the milling balls and inner surface of steel barrel. The yield of powder's working fraction (less than 300 μm size) depends considerably on oxide powder composition; moreover, it is observed the obvious tendency of decreasing of the yield with the increasing of zirconia content in oxide.

Powder, obtained by mechanical alloying, corresponds to initial steel with provision for its alloying by oxides (Fig. 2).

Element	Content, wt.%	Content, at.%
Si K	0.45	0.89
Ti K	0.57	0.65
Cr K	18.79	19.92
Mn K	1.62	1.63
Fe K	67.97	67.10
Ni K	10.15	9.53
Y L	0.35	0.22
Zr L	0.10	0.06
Total	100.00	100.00

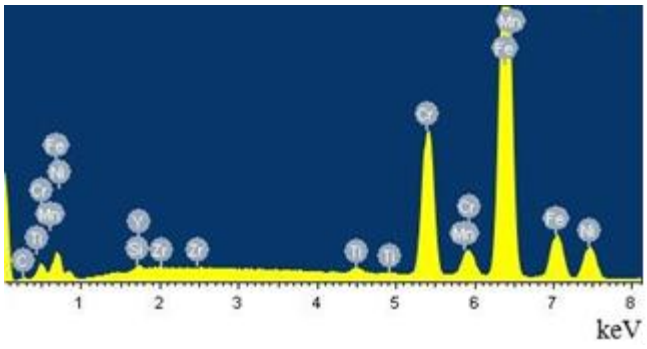

Fig. 2. Composition of steel particle after mechanical sintering with 0.5% of oxide of composition Y_2O_3-20 mol.% ZrO_2 during 4 hours (according to data of microanalysis)

Microstructure investigation showed that particles were represented as quite dense formations without visible boundaries and with a certain quantity of micropores with size from several fractions of micron to few microns.

As the result of characteristic radiation data collection it has been found, that all basic elements (Fe, Cr, Ni, Zr, Y, Mn and Si) had been distributed uniformly by cross section of particles.

Spherical particles ("balls") diameter size of 2…3 mm, obtained by mechanical alloying of fast quenched steel strips and oxide powder (with composition 80 mol.% Y_2O_3-20 mol.% ZrO_2) during 10 hours, were selected for electron-microscopic study. These particles were annealed at 1200 °C during 1 hour, squashed and annealed again. EM images of the structure and treatment results are shown in Fig. 3.

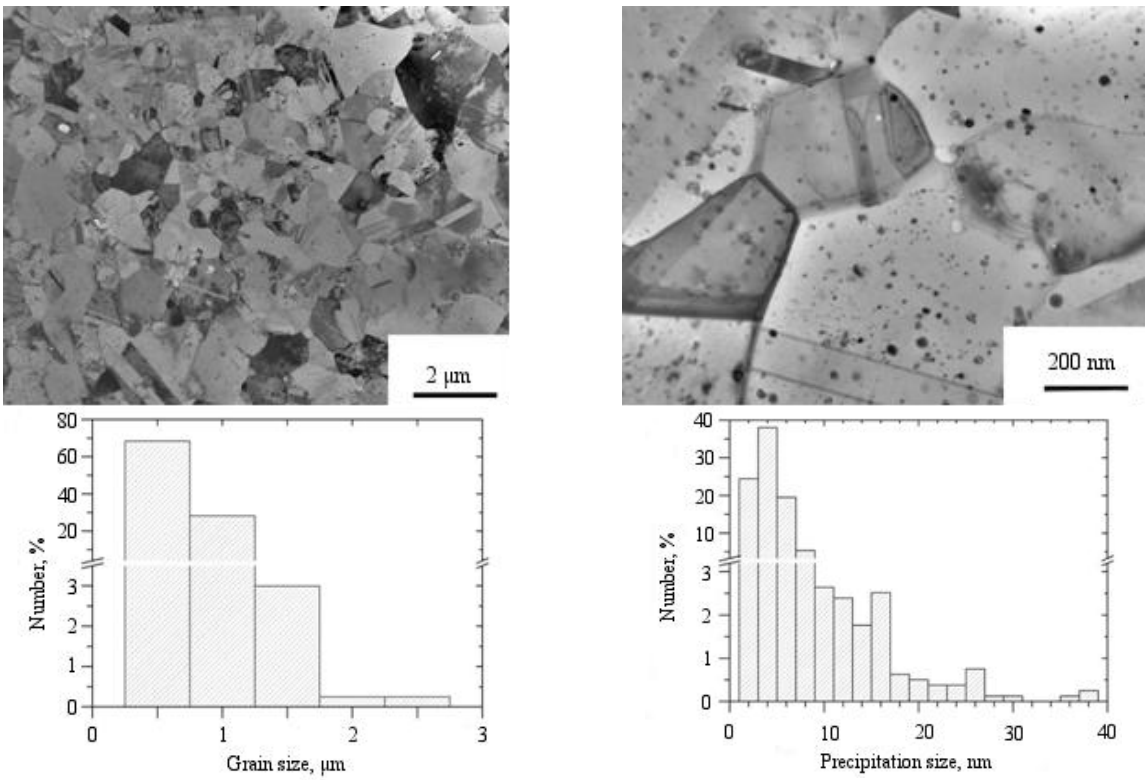

a *b*

Fig. 3. Structure of steel spherical particle ("ball"), obtained by mechanical synthesis, pressed and annealed at 1200 ºC: a – grains structure and grain size distribution; b – precipitates appearance and size distribution

As can be seen, there are a lot of fine precipitates inside of grains. Electron microprobe analysis had showed (Fig. 4) that precipitates contain titanium, yttrium, zirconium, oxygen and some other elements. Supposedly they have composition $Y_2(Ti, Zr)O_5$ but this result must be clarified. Besides the fine precipitates there is also a low quantity of larger particles size of up to 100 nm. According to microanalysis data these particles are titanium oxycarbonitrides and titanium oxides.

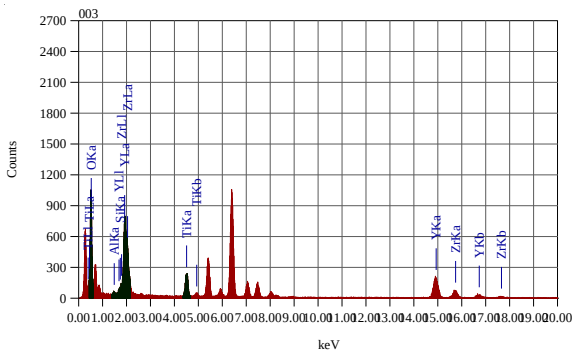

Fig. 4. Microanalysis of fine precipitates composition in a steel "ball" alloyed by yttrium-zirconium oxide

The results of ODS steel 08Cr18Ni10Ti powders X-ray diffraction data analysis on different production stages are represented below. The example of powder diffraction patterns in the initial state (after mechanical alloying) and after annealing are shown in Fig. 5.

As can be seen from Tabl. 2, mechanically alloyed steel contains austenitic and ferritic phase approximately in equal parts for all compositions of the oxide nanopowder. Lattice parameters of austenitic phase and mechanically induced ferritic are practically independent on oxide powder composition, but austenite lattice parameter higher than in basic steel (i. e. non-alloyed by oxides). This can be indicating that yttrium and/or zirconium atoms, which the atomic radii are significantly higher than the iron one, are embedded in the austenite lattice. Furthermore, increase of austenite lattice parameter can be related with implantation of oxygen atoms into the lattice. In other words, data on lattice parameter of oxide alloyed steel confirm the assumption about "break up" or dissociation of nanooxides during the high-energy grinding process and atoms implantation into the steel lattice. The decrease of

austenite lattice parameter after annealing (see Tabl. 1) confirms this assumption. This can be due to formation of oxide precipitates, which connect the "large" substitution yttrium and zirconium atoms with interstitial oxygen atoms.

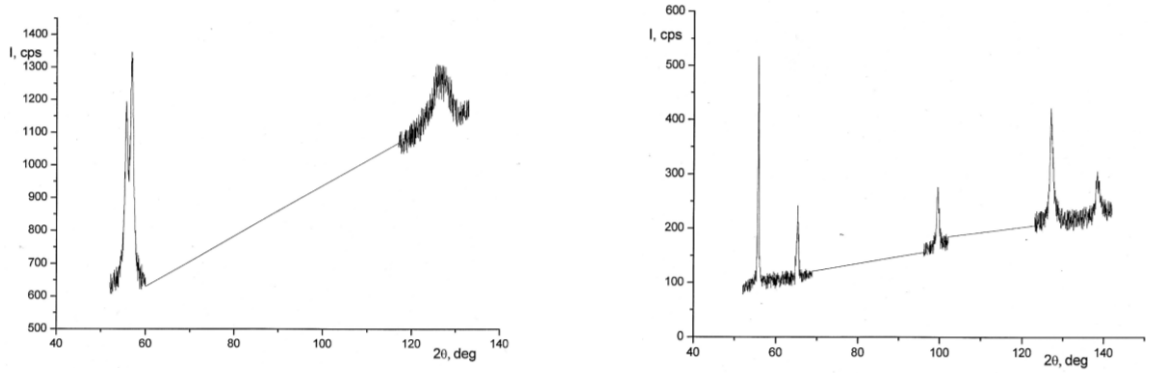

a *b*

Fig. 5. Diffraction patterns of steel powder mechanically alloyed by nanooxides of composition 80 mol.% Y_2O_3-20 mol.% ZrO_2:
a – initial state; b – after annealing at temperature 800 °C during 1 hour

Table 2

Phase composition and structure parameters of 08Cr18Ni10Ti steel powders, mechanically alloyed by nanooxides of different composition in two conditions: after grinding during 4 hours and subsequent annealing at 800 °C (initial equiaxial powders of steel are obtained by mechanic abrasion)

Alloying oxide composition		Phase	Composition, wt.%	Lattice parameter, Å	Crystallite size, nm	Microstrains
After grinding	8% Y_2O_3+92% ZrO_2	austenite	58.5	3.5968	39.6	$8.54 \cdot 10^{-3}$
		ferrite	41.5	2.875	–	–
	20% Y_2O_3+80% ZrO_2	austenite	42.7	3.5978	16.1	$6.23 \cdot 10^{-3}$
		ferrite	57.3	2.876	–	–
	80% Y_2O_3+20% ZrO_2	austenite	48.1	3.5988	14.8	$6.29 \cdot 10^{-3}$
		ferrite	51.9	2.876	–	–
Annealing 800 °C, 1 h	8% Y_2O_3+92% ZrO_2	austenite	100	3.5893	60.9	$1.34 \cdot 10^{-3}$
	20% Y_2O_3+80% ZrO_2	austenite	100	3.5886	100.3	$1.83 \cdot 10^{-3}$
	80% Y_2O_3+20% ZrO_2	austenite	100	3.5885	69.2	$2.81 \cdot 10^{-3}$

As to substructure parameters we must note the considerable decreasing of crystallite size and inessential decreasing of the microstrains level with the increase of yttrium content in the base oxide. The cause of these variations is not clear and further investigations are needed.

Besides the variation of lattice parameters the annealing of mechanically alloyed powders causes the 2…6 times increasing of crystallite size and decrease of the microstrains level in the same range. Unfortunately the correlation between these variations and oxide powder composition wasn't determined.

It was found (Tabl. 3) that the time of grinding doesn't influence significantly on phase composition of steel powder, but after grinding during 1 hour the content of mechanically induced ferrite occurs to be higher than for larger grinding time. Austenite and ferrite lattice parameters, also as the crystallite size, practically independent on the grinding time. At the same time the microstrains level in austenite and ferrite increases with the grinding time increasing.

Table 3

Influence of grinding time on phase composition and structural parameters of 08Cr18Ni10Ti steel powders, mechanically alloyed by nanooxides of composition 80 mol.% Y_2O_3-20 mol.% ZrO_2. (Fragments of initial steel ribbons after annealing were used)

Grinding time	Phase	Weight fraction, %	Lattice parameter, Å	Crystallite size, nm	Microstrains level
1 hour	austenite	66.9	3.600	13.4	$2.29 \cdot 10^{-3}$
	ferrite	33.1	2.873	15.4	$3.22 \cdot 10^{-3}$
2 hours	austenite	74.1	3.598	12.5	$3.85 \cdot 10^{-3}$
	ferrite	25.9	2.875	14.6	$4.17 \cdot 10^{-3}$
10 hours	austenite	75.3	3.595	11.9	$4.04 \cdot 10^{-3}$
	ferrite	24.7	2.876	18.2	$5.60 \cdot 10^{-3}$

STRUCTURAL CHARACTERISTICS OF ODS STEEL RIBBONS

Nano-sized powder 80 mol.%Y_2O_3-20 mol.%ZrO_2 (see Tabl. 1) was used as oxide on mechanical alloying and fast quenched ribbons were used as steel. Diffraction patterns, collected from rolled and annealed steel ribbons, are shown in Fig. 6. Results of diffraction patterns treatment are presented in Tabl. 4.

As it can be seen form table, after rolling two phases – austenite and ferrite are present either in initial steel as in ODS steel. Austenitic phase is textured (see Fig. 6,a), crystallographic planes (110) oriented parallel to rolling plane. Time of powder grinding influences insignificantly on lattice parameters and microstrains level in austenite and ferrite, but it is observed that the austenite crystallite size decreases with increasing of grinding time. It must be noted that the crystallite size and microstrains level in the initial steel are approximately the same as in ODS steel ribbons.

After annealing at T = 800 °C either phase composition as crystallite size and microstrains level changed considerably. Thus, in some specimen ferrite completely disappeared, in others its fraction appeared insignificantly.

Intensity relation of diffraction lines corresponds (see Fig. 6,b) to non-textured condition. Austenite lattice parameter is equal to the value before annealing within the error limits. Crystallite size of austenite increased in 3 times, and the microstrains level decreased in 1.5…3 times. At the same time in specimens with some ferrite quantity microstrains level is obviously higher ($2.8 \cdot 10^{-3}$) than in non-ferrite one ($(5.2…7.5) \cdot 10^{-4}$).

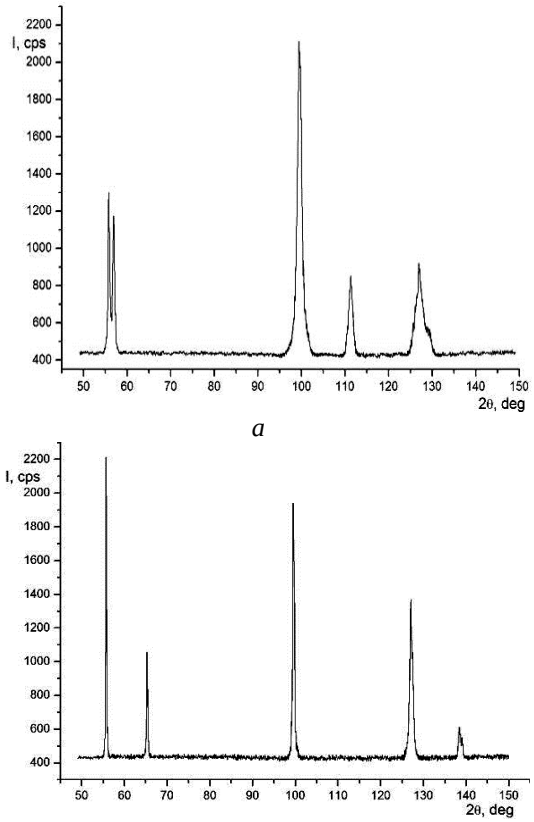

Fig. 6. Diffraction patterns of ODS steel ribbons after rolling (a) and annealing (b)

Table 4

Phase composition and structural parameters of initial steel ribbons and ODS steel ribbons (80 mol.% Y_2O_3-20 mol.% ZrO_2 nanooxides alloyed)

Condition	Phase	Weight fraction, %	Lattice parameter, Å	Crystallite size, nm	Microstrains level
Initial steel, rolling	austenite	75	3.587	41.1	$2.86 \cdot 10^{-3}$
	ferrite	25	2.873	58.6	$2.75 \cdot 10^{-3}$
Initial steel, rolling and annealing (800 °C, 1 h)	austenite	96.3	3.5880	124.4	$1.09 \cdot 10^{-3}$
	ferrite	3.7	2.872	101.4	$1.60 \cdot 10^{-3}$
ODS steel, grinding 1 h, rolling	austenite	–	3.588	51.7	$1.06 \cdot 10^{-3}$
	ferrite	–	2.874	64.4	$2.56 \cdot 10^{-3}$
ODS steel, grinding 1 h, rolling and annealing (800 °C, 1 h)	austenite	100	3.5868	169.4	$7.47 \cdot 10^{-4}$
ODS steel, grinding 2 h, rolling	austenite	–	3.589	46.2	$1.86 \cdot 10^{-3}$
	ferrite	–	2.877	32.8	0
ODS steel, grinding 2 h, rolling and annealing (800 °C, 1 h)	austenite	100	3.5877	149.6	$5.17 \cdot 10^{-4}$
ODS steel, grinding 4 h, rolling	austenite	55.1	3.5909	34.0	$5.78 \cdot 10^{-3}$
	ferrite	44.9	2.874	–	–
ODS steel, grinding 4 h, rolling and annealing (800 °C, 1 h)	austenite	92.9	3.5853	284.0	$2.84 \cdot 10^{-3}$
	ferrite	7.1	2.796	–	–

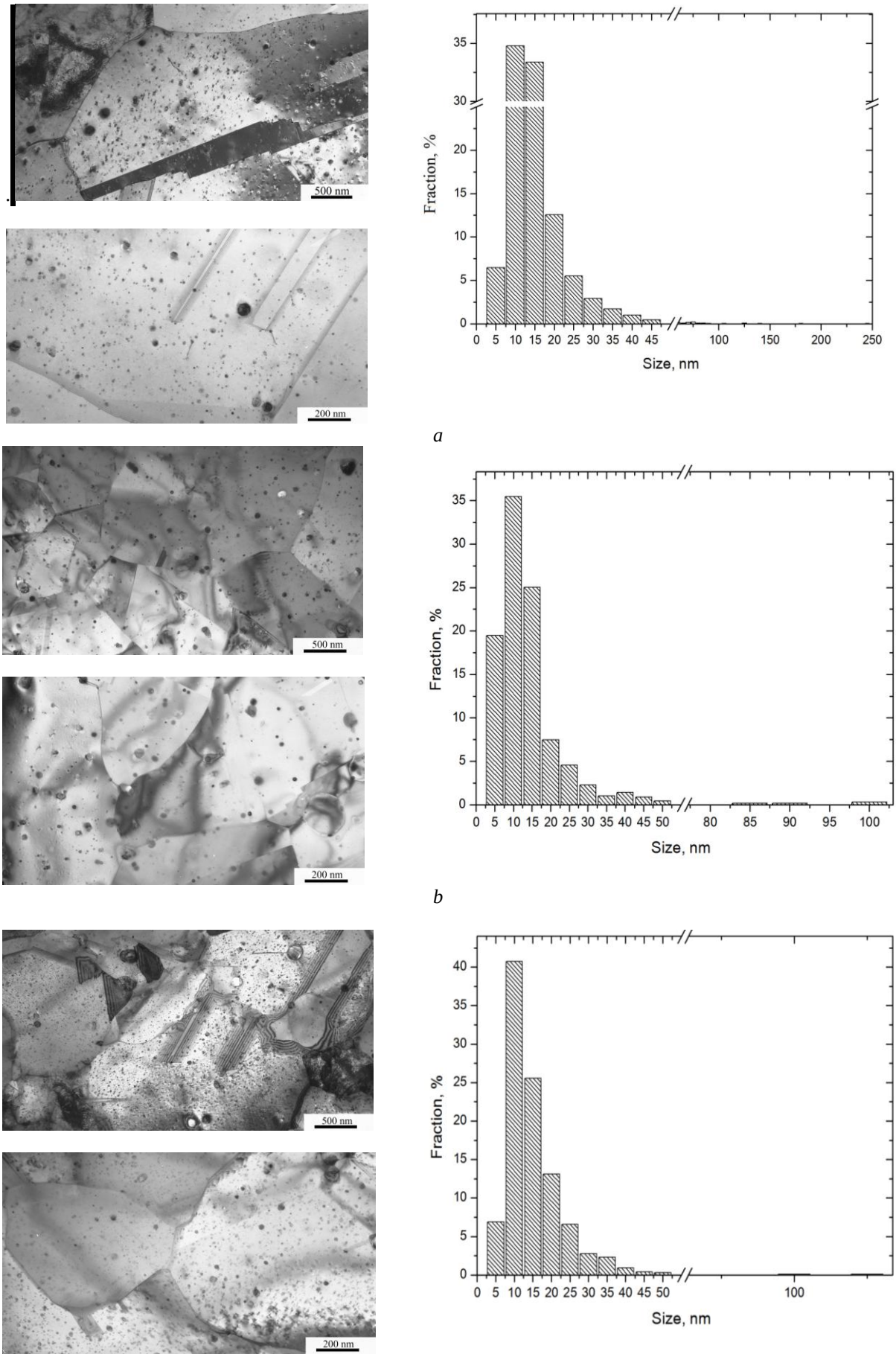

a

b

c

Fig. 7. Microstructure of steel ribbon specimens, alloyed by nanooxides of different composition and size distribution of oxide precipitates: a – alloying oxide $8Y_2O_3$-$92ZrO_2$; b – alloying oxide $20Y_2O_3$-$80ZrO_2$; c – alloying oxide $80Y_2O_3$-$20ZrO_2$ (numbers are molar percent)

EM microstructure studies were performed on ribbons prepared from mechanically alloyed powder obtained by grinding during 4 hours. Main purpose of microstructure studies was on establishment of quantitative microstructure parameters, which determinate mechanical characteristics of steel and its behavior under the irradiation. Those characteristics are: grain size, precipitations density, its average size and size distribution.

Microstructure images of 08Cr18Ni10Ti steel, alloyed by Y_2O_3-ZrO_2 nanooxides, and oxide precipitates size distribution histograms are shown on Fig. 7. Grain structure was the same approximately for all samples, average grain size was 1.2…2.0 μm (Tabl. 5). Significant concentration of precipitates and its near-uniform distribution are observed for all samples. This is a dominant condition on ODS steel production.

Precipitations size varied from some of nanometers to hundreds of nanometers, but the last were a few orders less, thus, its contribution to concentration and average size was negligible. Note, that calculations were performed on large data array (more than 1000 precipitates per composition). Table 5 contains generalized data on precipitates characteristics of specimens with different composition. As it is seen from table the best characteristics are observed in ODS steel specimen, obtained using $80Y_2O_3$-$20ZrO_2$ nanopowder. In this specimen minimal average grain and precipitates size, maximal precipitations density and most narrow its size distribution are observed. Large precipitations (size of more than 50 nm) are practically absent (see Fig. 7,b). Determination of formed oxides composition is a goal of the following investigations.

Table 5

Microstructure characteristics of ribbons, alloyed by oxides of different composition

Alloying oxide composition, mol.%	Average grain size, μm	Average oxide precipitates size, μm	Density of precipitates, cm^{-3}
$8Y_2O_3$-$92ZrO_2$	2	13	$1.7 \cdot 10^{15}$
$20Y_2O_3$-$80ZrO_2$	1.5	13	$4.5 \cdot 10^{15}$
$80Y_2O_3$-$20ZrO_2$	1.2	10	$7.3 \cdot 10^{15}$

MECHANICAL PROPERTIES MECHANICAL PROPERTIES

Mechanical testing results of initial and ODS steel ribbons, annealed on final stage at 1000 °C, are presented in Tabl. 6. Fast-quenched steel ribbons and $80Y_2O_3$-$20ZrO_2$ oxide nanopowders were used for mechanical alloying. 700 °C testing temperature was selected as bench mark, for which requirements on mechanical properties of FE claddings for fast reactors are known.

Table 6

Mechanical properties of base steel 08Cr18Ni10Ti and steel alloyed by nanooxides with composition $80Y_2O_3$-$20ZrO_2$

Steel	Mechanical properties on different temperatures testing						
	$\sigma_{0.2}$, MPa		σ_B, MPa		δ, %		H_μ, MPa
	20 °C	700 °C	20 °C	700 °C	20 °C	700 °C	20 °C
Initial	242	158	725	279	55.0	19.7	2120
ODS	510	370	799	415	40.5	12.0	2700

As it can be seen strength characteristics of ODS steel at both temperatures are considerably higher than that of initial steel. Effect of nanoparticles strengthening is strongly pronounced at temperature 700 °C. So, if conditional yield strength $\sigma_{0.2}$ at room temperature increases due to alloying in 2.1 times, then it increases in 2.3 times at temperature 700 °C. Tensile strength σ_B at these temperatures increases in 1.1 and 1.5 times, respectively.

There are few publications on austenitic ODS steels. There are more less publications, where mechanical properties of these steels were investigated at near-operating temperatures. Thus, authors [11] cited data on mechanical properties of AISI 316L ODS steel at 20 °C and 700 °C temperatures. These properties are lower than we have obtained. Evidently, the reason is smaller oxide precipitates size and more uniform size distribution in our samples.

CONCLUSION

Features of austenitic 08Cr18Ni10Ti ODS steel mechanical alloying by Y_2O_3-ZrO_2 nanooxides were studied. It is shown that powders contain austenitic and ferritic phases after mechanical alloying. Moreover, the quantity of mechanically induced ferrite mainly depends on quality of the initial steel before alloying. In the case of equiaxial powders, obtained by mechanical abrasion, the quantity of ferrite is considerably higher than on using fast-quenched ribbons. Austenitic and ferritic phases of steel powders, mechanically alloyed by nanooxides, have approximately the same crystallite size. But it is observed the tendency of crystallite size decreasing and increasing of the microstrains level with

the yttria content increasing in basic oxide nanopowders. Annealing at temperatures above 800 °C leads to austenization, and, at the same time, crystallite size increases and microstrains level decreases.

Structural investigations of mechanically alloyed steel powders showed that even in coarse particles after thermal treatment there was a considerable amount of small oxide precipitates with complex composition. These precipitates contain yttrium, titanium, zirconium and other elements. In the ODS steel ribbons after the final thermal treatment austenitic matrix phase is observed. Complex oxide precipitates density varies within $(1.7…7.3)\cdot10^{15}$ cm^{-3} range and the average size is near 10 nm. Moreover, the highest density of precipitates, the lower mean size and higher homogeneity of its size distribution were detected in specimen, alloyed by 80 mol.% Y_2O_3-20 mol.% ZrO_2 nanooxides.

Strength characteristics of ODS steel, obtained by 80 mol.% Y_2O_3-20 mol.% ZrO_2 nanooxides alloying, are significantly higher than the initial steel ones. Especially substantial gain is observed at high temperatures (700 °C), where the yield strength of ODS steel is 2.3 times higher than for initial steel 08Cr18Ni10Ti. At the same time, ductility decreases slightly, but remains on sufficient level for technological and operational purposes.

REFERENCES

1. R.L. Klueh and A.T. Lelson. Ferritic/Martensitic Steels for Next-Generation Reactors // *J. Nucl. Mater*. 2007, v. 371(1-3), p. 37-52.
2. A. Ramar, N. Baluc, R. Schaublin. On the lattice coherency of oxide particles dispersed in EUROFER97 *// J. Nucl. Mater*. 2009, v. 386-388, p. 515-519.
3. C. Liu, C. Yu, N. Hashimoto, S. Ohnuki, M. Ando, K. Shiba, S. Jitsukaw. Micro-structure and microhardness of ODS steels after ion irradiation // *J. Nucl. Mater*. 2011, v. 417, p. 270-273.
4. V.V. Brykh, V.M. Voyevodin, O.S. Kalchenko, V.V. Melnichenko, I.M. Neklyudov, V.S. Ageev, A.O. Nikitina. Swelling of dispersion strengthened by yttrium oxides steel 08Cr18Ni10Ti, irradiated by heavy ions // *PAST. Series "Physics of radiation defects and radiation materials science*". 2013, N 2(84), p. 23-30.
5. S. Ukai, M. Harada, H.Okada. Alloying design of oxide dispersion stengthened ferritic steel for long life FBRs core materials // *J. Nucl. Mater.* 1993, v. 204, p. 65-73.
6. V.V. Sagaradze, V.I. Shalaev, V.L. Arbuzov, B.N. Goshchitskii, Yun Tian, Wan Qun, Sun Jiguang. Radiation resistance and thermal creep of ODS ferritic steels // *J. Nucl. Mater*. 2001, v. 295, p. 265-272.
7. C. Cayron, E. Rath, I. Chu, S. Launois. Microstructural evolution of Y_2O_3 and $MgAl_2O_4$ ODS EUROFER steels during their elaboration by mechanical milling and hot isostatic pressing // *J. Nucl. Mater*. 2004, v. 335, p. 83-102.
8. T.S. Srivatsan, N. Narendra, J.D. Troxell. Tensile deformation and fracture behavior of an oxide dispersion strengthened copper alloy // *Materials & Design*. 2000, N 21 (3), p. 191-198.
9. O.M. Bovda, O.E. Dmitrenko, D.G. Malykhin, L.V. Onishchenko, V.M. Pelykh. Structure and properties of fast-quenched Zr-based alloys // *PAST. Series "Vacuum, pure materials, superconductors".* 2007, N 4, p.173-178.
10. Th.H. De Keijser, J.I. Langford, E.J. Mettemeijer, A.B.P. Vogels. Use of the Voigt function in a single-line method for the analysis of X-ray diffraction line broadening // *J. Appl. Cryst*. 1982, v. 15, p. 308-314.
11. Tae Kyu Kim, Chang Soo Bae, Do Hyang Kim, Jinsung Jang, Sung Ho Kim. Chan Bock Lee and Dohee Hahn, Microstructural observation and tensile isotropy of an austenitic ODS steel // *Nuclear Engineering and Technology*. 2008, v. 40, N 4, p. 305-310.

Article received 09.07.2014

СТРУКТУРА И СВОЙСТВА АУСТЕНИТНОЙ ДУО СТАЛИ 08Х18Н10Т

А.Н. Великодный, В.Н. Воеводин, М.А. Тихоновский, В.В. Брык, А.С. Кальченко, С.В. Старостенко, И.В. Колодий, В.С. Оковит, А.М. Бовда, Л.В. Онищенко, Г.Е. Сторожилов

С использованием механического легирования получены экспериментальные образцы аустенитной нержавеющей стали 08Х18Н10Т, дисперсно-упрочненной нанооксидами системы Y_2O_3-ZrO_2 различного состава. Изучена микроструктура образцов на разных стадиях получения в зависимости от состава легирующего оксида и условий механико-термической обработки, определены их структурные параметры (размер зерен, плотность и распределение выделений по размерам и др.). Измерены механические свойства лент и показано, что характеристики ДУО стали существенно выше по сравнению с обычной сталью, полученной по тем же режимам. Особенно существенное различие в условиях испытаний при 700 ºС, где увеличение условного предела текучести составляет 2,3 раза. Пластичность ДУО стали несколько ниже, чем у исходной, однако ее величина остается на уровне, достаточном для технологических и эксплуатационных целей.

СТРУКТУРА І ВЛАСТИВОСТІ АУСТЕНІТНОЇ ДЗО СТАЛІ 08Х18Н10Т

О.М. Великодний, В.М. Воєводін, М.А. Тихоновський, В.В. Брик, О.С. Кальченко, С.В. Старостенко, І.В. Колодій, В.С. Оковіт, О.М. Бовда, Л.В. Онищенко, Г.Є. Сторожилов

З використанням механічного легування отримані експериментальні зразки аустенітної нержавіючої сталі 08Х18Н10Т, дисперсно-зміцненої нанооксидами системи Y_2O_3-ZrO_2 різного складу. Вивчено мікроструктуру зразків на різних стадіях отримання залежно від складу легуючого оксиду та умов механіко-термічної обробки. Визначено структурні параметри стрічкових зразків (розмір зерен, щільність і розподіл виділень за розмірами та ін.). Виміряно механічні властивості стрічок при кімнатній температурі і при 700 ºС і показано, що характеристики ДЗО сталі істотно вищі в порівнянні із звичайною сталлю, отриманою за тими ж режимами. Особливо істотне це розходження в умовах випробувань при 700 ºС, де зростання умовної межі текучості становить близько 2,3 рази. Пластичність ДЗО сталі трохи нижча, ніж у вихідної, однак її величина залишається на рівні, достатньому для технологічних та експлуатаційних цілей.